Published in final edited form as:
Brain Behav Evol. 2014 ; 84(1): 19–30. doi:10.1159/000362431.

Evolution of the Central Sulcus Morphology in Primates

William D. Hopkins[a,b], **Adrien Meguerditchian**[c], **Olivier Coulon**[d], **Stephanie Bogart**[a,b], **Jean-François Mangin**[e], **Chet C. Sherwood**[f], **Mark W. Grabowski**[f], **Allyson J. Bennett**[g], **Peter J. Pierre**[h], **Scott Fears**[i,j], **Roger Woods**[i,j], **Patrick R. Hof**[k,l], and **Jacques Vauclair**[m]

[a]Neuroscience Institute, Georgia State University, Atlanta, Georgia 30302

[b]Division of Developmental and Cognitive Neuroscience, Yerkes National Primate Research Center, 954 Gatewood Road, Atlanta, Georgia 30322

[c]Laboratoire de Psychologie Cognitive, Aix-Marseille University/CNRS, UMR7290, Marseille, France

[d]Laboratoire des Sciences de l'Information et des Systèmes, Aix-Marseille Universite, Marseille, France

[e]LNAO, Neurospin, I2BM, CEA, Gif-sur-Yvette, France

[f]Department of Anthropology and Center for the Advanced Study of Hominid Paleobiology, The George Washington University, Washington, DC 20052

[g]Harlow Center for Biological Psychology, Psychology Department, University of Wisconsin, Madison, Wisconsin 53715

[h]Department of Behavioral Management, Wisconsin National Primate Research Center, Madison, Wisconsin 53115

[i]Center for Neurobehavioral Genetics, University of California, Los Angeles (UCLA), Los Angeles, California 90095

[j]Department of Neurology, University of California, Los Angeles (UCLA), Los Angeles, California 90095

[k]Fishberg Department of Neuroscience and Friedman Brain Institute, Mount Sinai School of Medicine, New York, New York 10029

[l]New York Consortium in Evolutionary Primatology, New York, New York 10029

[m]Department of Psychology, Research Center in Psychology of Cognition, Language & Emotion, Aix-Marseille University, Aix-en-Provence, France

Abstract

The central sulcus (CS) divides the pre- and post-central gyri along the dorsal-ventral plane of which all motor and sensory functions are topographically organized. The motor-hand area of the precentral gyrus or knob has been described as the anatomical substrate of the hand in humans.

Corresponding author: William D. Hopkins, Ph.D. Georgia State University, Neuroscience Institute & Language Research Center, P.O. Box 5030, Atlanta, Georgia 30302, Phone: (404) 727-8235, Fax: (404) 727-5852, whopkin@emory.edu.

Given the importance of the hand in primate evolution, here we examined the evolution of the motor-hand area by comparing the relative size and pattern of cortical folding of the CS surface area from magnetic resonance images in 131 primates including Old World monkeys, apes, and humans. We found that humans and great apes have a well-formed motor-hand area that can be seen in the variation in depth of the CS along the dorsal-ventral plane. We further found that great apes have relatively large CS surface areas compared to Old World monkeys. However, relative to great apes, humans have a small motor-hand area in terms of both adjusted and absolute surface areas.

Keywords

central sulcus; motor-hand area; hand functions; gyrification; cortical folding

During primate evolution, the cerebral cortex has become increasingly gyrified concomitant with enlargement in size. Humans show the greatest degree of cortical folding followed by apes, then the more distantly related monkeys and strepsirrhines [Rilling and Insel 1999b; Rogers et al. 2010; Zilles et al. 1989]. The central sulcus (CS) is a prominent cortical fold, one of the first to form in embryogenesis, which divides the pre- and postcentral gyri. Motor and sensory systems are represented along the dorsal-ventral axis of these two gyri, which are sometimes referred to as the “motor and sensory homunculi”. In Old Word monkeys and apes, the primary motor cortex (Brodmann's area 4) is located along the anterior bank of the central sulcus and extends onto the free surface of the precentral gyrus, whereas in humans the primary motor cortex is mostly restricted to the buried surface of the central sulcus [Sherwood et al. 2004]. In human and nonhuman primates, stimulation of the motor cortex in the mid portion of the precentral gyrus results in movement of the individual digits of the hand whereas stimulation in more ventral regions results in movements of facial musculature including the lips, eyes, vocal folds, and tongue [Bailey et al. 1950; Penfield and Boldrey 1936; Petrides et al. 2005].

Humans are distinct from other primates with respect to manual motor skills and control. Specifically, the human hand is distinguished from that of apes by shorter fingers relative to the thumb, increased robusticity of the thumb, and a wider range of movement at the wrist [Tocheri et al. 2008]. These modifications have resulted in increased opposability of the thumb and individual control of digits [Connolly 1998; Marzke 1996]. It has been hypothesized that with the advent of bipedalism in early humans, the hands were subsequently freed from participating in locomotor function and became increasingly involved in complex manipulative actions such as prehensile grasping, tool use, tool making, and gestural communication [Bradshaw 1997; Corballis 2002; Marzke 1997; Young 2003].

Because of the importance of increasing motor control of the hand found in primate evolution [Castiello 2005], we sought to examine the evolution of the surface area and folding of the CS in primates. Comparative examination of the dorsal-ventral variation in the surface area and depth of the CS in different primate species was of specific interest. Recent studies in humans and chimpanzees have identified an anatomical landmark in the middle portion of the CS referred to as the motor-hand area, or KNOB [Hopkins and Pilcher 2001;

Yousry et al. 1997]. The KNOB has been described as an epsilon- or omega-shaped formation, although there is some variation in its appearance [Caulo et al. 2007]. It has been suggested that the formation of the KNOB is attributable to the presence of a buried gyrus that connects the pre- and post-central gyri referred to as the “pli de passage fronto-parietal moyen” (PPFM), originally described by Broca [Alkadhi and Kollias 2004; Boling et al. 1999]. In the presence of the PPFM, the central portion of the CS has to fold over this gyrus, which results in the formation of the KNOB. In humans, functional imaging studies have shown that individual movement of the digits and wrist are spatially represented along the contour of the KNOB, suggesting that this region represents the cortical substrate of the hand [Boroojerdi et al. 1999; Pizzella et al. 1999; Sastre-Janer et al. 1998]. Indeed, though rare, occasionally the PPFM can project to the surface of the cortex resulting in a bifurcation of the CS [Alkadhi and Kollias 2004; Boling et al. 1999]. Interestingly, where the split in the CS occurs divides the motor representation of the wrist from the individual digits, further implicating this region as the cortical region controlling digit use. In chimpanzees, a positron emission tomography study showed activation in the KNOB region in the hemisphere contralateral to the hand used during a reach-and-grasp task [Hopkins et al. 2010b], suggesting that the KNOB may similarly represent the cortical substrate of the hand in this species. Finally, in both humans and chimpanzees, anatomical asymmetries in the KNOB have been linked to individual differences in hand preference and skill at the level of gross morphology [Amunts et al. 1996; Foundas et al. 1998; Hopkins and Cantalupo 2004; Kloppel et al. 2010; Li et al. 2009] and histology [Sherwood et al. 2010; Sherwood et al. 2007]. These findings reinforce the view that the motor hand area of the precentral gyrus may represent the neural substrate of the hand and possibly handedness.

In the current study, we sought to examine the evolution of CS size and morphology, particularly for the KNOB, across primates in relation to the size of the cerebral cortical surface. The motor skills of apes have been demonstrated to exceed those of other primates [Christel 1994; Pouydebat et al. 2009]; thus, we hypothesized that the morphology and folding pattern of humans and apes would differ from those of more distantly related Old World monkeys. Given the elaboration of manual motor skill in humans, we also aimed to determine whether the human CS shows modification of its morphology or surface area as compared to apes. To test these hypotheses, magnetic resonance images (MRI) of the brain were obtained from primates representing 10 species covering 30 millions years of evolutionary history (since the divergence of the last common ancestor of Old World monkeys and humans). From the MRI scans, we initially quantified the surface area and depth of the CS using BrainVisa software (see below). BrainVisa analyzes on cortical folding patterns of the brain and uses sulcus-based morphometry [Mangin et al. 2004], which differs from manual tracing approaches because it quantifies both the surface area and depth of the sulci rather than solely the linear length of the outer contour of the sulcus. The use of the BrainVisa's morphometry tools for quantifying brain specialization is particularly interesting in comparison to manual tracing approaches. Indeed BrainVisa's tools involve automatic processes for analyzing the brain images which prevents from variation of human judgments related with manual tracing and minimize then potential observer bias.

Methods

Subjects

Magnetic resonance images (MRI) were obtained from a total of 131 primates including humans (*Homo sapiens*, n = 11, all males), chimpanzees (*Pan troglodytes*, *n* = 19, 10 males and 9 females), bonobos (*Pan paniscus*, *n* = 12, 7 males and 5 females), gorillas (*Gorilla gorilla*, *n* =18, 13 males and 5 females), orangutans (*Pongo pygmaeus*, *n* = 15, 9 males and 6 females), gibbons (*Hylobates lar*, *n* = 4, 2 males and 2 females), baboons (*Papio anubis*, *n* = 4, 2 males and 2 females), vervet monkeys (*Chlorocebus aethiops sabaeus*, *n* = 12, all females), rhesus monkeys (*Macaca mulatta*, *n* = 21, 16 males and 5 females) and bonnet monkeys (*Macaca radiata*, *n* = 16, 8 males and 8 females). For the humans, gibbons, vervet, rhesus and bonnet monkeys, all the MRI scans were obtained *in vivo* while a combination of *in vivo* (IV) and post-mortem (PM) scans made up the baboon (2 PM, 2 IV), orangutan (4 IV, 11 PM), gorilla (2 IV, 16 PM), chimpanzee (9 IV, 10 PM) and bonobo (4 IV, 8 PM) samples. All PM brains were collected following the naturally occurring death of the subjects. Thus, no subjects were sacrificed for the purposes of this study. In humans, the absence of anatomical MRI scans in females prevents us to evaluate the potential gender effect on the variation of the CS within a comparative framework with the other primate species. The vervet monkeys were members of the Vervet Research Colony at UCLA [Fears et al. 2009]. The bonnet and rhesus monkeys were housed at Wake Forest University Primate Center. For all species, the scanning procedures were performed under the guidelines of state and federal laws, the U.S. Department of Health and Human Services and institutional animal care and use committees.

Image Collection and Procedure

This study was opportunistic in terms of availability of *in vivo* and post-mortem MRI scans. Thus, as noted above, the magnets and scanning protocols were not identical in all species. Further, in the case of humans, our sample was restricted to males. This presents some limitations for certain comparative analyses because variation in magnet strength and/or scanning protocol can influence the signal strength and sensitivity in contrast between grey matter, white matter and CSF. Moreover, shrinkage in tissue due to fixatives can result in some distortion in size of various structures. However, in all of the comparative analyses of CS surface area and depth, the individual values were adjusted for whole brain measures taken from the same scan either by calculating a ratio measure or by regression. Thus, inherent differences in grey matter, white matter and CSF due to the scanning protocols or magnet strength were standardized within individuals when quantifying the surface area and depth of the CS (also see Discussion).

For *in vivo* MRI scans in all species except humans, subjects were first immobilized by ketamine injection as appropriate for the species and subsequently anaesthetized with propofol (chimpanzees), midazolam and ketamine (vervets) or isofluorane (rhesus and bonnet macaques). The subjects remained anaesthetized for the duration of the scans as well as the time needed to transport them between their home cage and the imaging facility (total time ∼ 2 h, MRI acquisition time ranging from 36-60 minutes). All scans were examined at the time of acquisition and any image with artifact was excluded in the subsequent image

processing. After completing MRI procedures, the subjects were temporarily housed in a single cage for 6–12 h to allow the effects of the anesthesia to wear off, after which they were returned to their home cage. The archived MRI data were transferred to a PC running BrainVisa software for post-image processing. To provide an unbiased collection of human subjects, a heterogeneous sample set (n = 11) was randomly assembled from the BrainVisa database. All MR images were previously processed through the software before including them in our analyses. As such, the scans originated from many different scanners and protocols over the span of 20 years using an approximate gradient echo protocol (inversion time = 500 ms, pulse repetition = 10 ms, echo time = 2 ms, and a 256 × 256 matrix). For the post-mortem scanning, either 4.7 or 7T magnets were used and T2-weighted images were collected in the transverse plane using a gradient echo protocol (pulse repetition = 22.0 s, echo time = 78.0 ms, number of signals averaged = 8-12, and a 256 × 192 matrix reconstructed to 256 × 256).

Image Processing

The sequence of processing steps performed on the images is shown in Figures 1a to 1h. The pipeline of processing used to extract central sulcus from the raw T1-weighted image derives from a pipeline initially dedicated to the human brain and freely distributed as a BrainVISA toolbox (http://brainvisa.info) [Mangin et al. 2004]. The human-dedicated pipeline has been used previously for at least 5000 different subjects. Some tuning of this pipeline was required to account for specificities of the nonhuman primate anatomy as well as the different protocols used to acquire the images in the *in vivo* and post-mortem brains. Notably, for the post-mortem MRI scans, we had to invert the intensities corresponding to grey and white matter in order for BrainVISA to run properly. The pipeline processing steps proceeded in the following manner: First, correction of the spatial inhomogeneities of the signal, which prevent direct association between the signal intensity and the nature of the tissue, were performed. The estimation of the spatially smooth bias field used to restore the signal intensity was performed via minimisation of the signal entropy [Mangin 2000]. After correction, each tissue intensity distribution was stable across the brain (see Fig. 1b). Second, automatic analysis of the signal histogram and mathematical morphology was then used to compute a binary mask of the brain (see Fig. 1c). This approach is built on the fact that the brain is surrounded by dark areas corresponding to skull and cerebrospinal fluid (CSF). Therefore, once the range of intensities corresponding to brain tissue had been defined by histogram analysis, brain segmentation mainly amounts to splitting the connections with external structures like the optic nerves. For the chimpanzee anatomy, some specific tuning had to be applied relative to the human-dedicated processing performed by BrainVISA [Mangin et al. 1998]. For some chimpanzees, indeed, the largest object in the image after splitting connections turns out to be the muscles. Hence, in order to reliably select the brain, we had to introduce an additional constraint relative to the localization of the brain in the middle of the head. Once the brain mask had been defined, the mask was split into three parts corresponding to hemispheres and cerebellum (see Fig. 1d) [Mangin et al. 1996].

After a mask has been defined for each hemisphere, a negative mould of the white matter was computed [Mangin et al. 1996]. The outside boundary of this mould results from a 5-

mm “closing” of the masked hemisphere. Here, “closing” is an operation of Mathematical Morphology used to analyze shapes: the mask of the hemisphere is first “dilated” then “eroded” which results in deleting the folds that are less than 5mm wide. The inside boundary is the grey/white interface computed with topology preserving deformations assuring the spherical topology of the mould (see Fig. 1e). Imposing the actual topology of the cortex to the mould prevents the detection of spurious folds resulting from noisy data [Mangin et al. 1995]. The mould is finally skeletonized in order to detect the cortical fold as crest surfaces of the 3D MR image located inside the mould [Mangin et al. 2004]. Skeletonization is another standard technique in Mathematical Morphology. An object is eroded until losing its thickness: for example, a door would become a flat 2D surface or a ball with a cavity would become a sphere. The crest surfaces stem from a morphological watershed process iteratively eroding the 3D mould from the lightest intensities to the darkest intensities. Topological constraints guarantee that the resulting surfaces have no holes. The end result is a set of topologically elementary surfaces located along the darkest part of the fold corresponding to CSF (see Fig. 1f-g). These elementary surfaces are split further when a deformation of the deepest part of the fold indicates the presence of a buried gyrus. The clues allowing the detection of buried gyri are embedded in the curvature of the grey/white interface [Mangin et al. 2004]. Indeed, a buried gyrus leads to a horse saddle shape in the depth of the grey/white interface, which results in a negative Gaussian curvature providing these clues. Finally, the cortical folds comprising the sulci are presented in the 3D visualization graph (Fig 1h) and the folds making up the central sulcus were selected manually by the user. The authors simply chose the central sulcus among other folds. Note that while this selection can be ambiguous in the human brain, because of the variability of fold interruptions, no error can occur with other primates. The extracted CS from representative species in this study is shown in Figure 2.

Cortical Measures

For the CS, two primary measures were obtained including the surface area and the depth of the CS along the entire dorsal-ventral plane (see Figure 3 and 4a). Surface area (mm^2) was measured independently by the software and reflected the area of the CS as a function of the depth and length of the sulcus. Using BrainVisa, we also computed the total folded cortical sulci surface area (mm^2) for each hemisphere and subject, which includes only the surface area within cerebral sulci, excluding the gyral cortex. The total cortical folded surface area excluded the cerebellum and brain stem regions. This measure allowed us to compare the CS surface area in each species after adjusting for total folded cortical surface area. To compute the relative surface area of the CS, we divided the surface area of the CS by the total folded cortical surface area and multiplied by 100 (Percent_CS). This measure indicated the percentage of the total surface area of the brain that was comprised of the CS.

Because interspecific data should not be considered independent - i.e. relationships between species lead to relationships between data points [Felsenstein 1985] - two approaches where used to incorporate phylogenetic information in the analysis. First, we calculated phylogenetic ANOVAs [Garland et al. 1993] using the phytools R package [Revell 2011]with monkeys as one group and apes as the other, to test if there was an effect of a grade-shift on Percent_CS when phylogeny was taken into account. In addition, to explore

allometric scaling, we calculated both ordinary least squares regression coefficients and phylogenetic generalized least squares (PGLS) [Grafen 1989; Martins and Hansen 1997] to test for the relationship between CS surface area and total folded cortical surface area (with CS surface area subtracted) assuming a Brownian Motion model of trait evolution. All data in regression analyses were natural logged. We used the PGLS function the package Caper [Orme 2012]. All phylogenetic analyses were conducted using R 3.0.2 [Team 2011].

Central Sulcus Parameterization and Fold Depth

For each subject, the CS was standardized into 100 equally spaced sections along the dorsal-ventral axis and the depth of the sulcus at each point was quantified. The procedure can be briefly summarized as follows: a coordinate system is computed on the sulcus that indicates the position of each point relative to its depth (x coordinate) and its position along the sulcus between the dorsal and ventral extremities (y coordinate), as illustrated in Figure 4b and 4c. At each position, y=0 through100 along the sulcus length, the depth is defined as the length of the corresponding y iso-coordinate line (see Figure 4d). Various publications provide more technical details about this procedure [Coulon et al. 2006; Cykowski et al. 2008; Davatzikos and Bryan 2002; Hopkins et al. 2010a].

Data Analysis and Quantification of the Pli-de-Passage

To explore the variation in the central CS region further, we quantified the CS depth corresponding to the “pli de passage fronto-parietal moyen” (PPFM) using previously described methods [Coulon et al. 2006; Cykowski et al. 2008; Hopkins et al. 2010a]. Because the PPFM was only identifiable in the great apes and humans (see below), these analyses were restricted to those species. Briefly, we recorded the largest depth measure that was superior (SP) and inferior (IP) to the central location of the CS (location 50) (Figure 4d). We then recorded the shallowest CS depth (PPFM) between the SP and IP locations (Figure 4d). The maximum depth of the PPFM was then computed following the formula: *[PPFM_max = ((depth(IP)+depth(SP))2.0) -depth(PPFM)]*. This measure reflected the magnitude of cortical folding of the central CS region relative to the superior and inferior points in each subject and species and was used to quantify the region, which included the motor hand area. For all analyses, α was set to 0.05 and, when necessary, post-hoc tests were conducted using Tukey's Honestly Significant Difference (HSD) tests.

Results

Central Sulcus Surface Area

In the initial analysis, we compared the Percent_CS measure between species. A one-way analysis of variance revealed a significant main effect for species ($F_{(9, 121)} = 20.37$, $p < 0.001$). The mean Percent_CS score for each species is shown in Figure 5. Post-hoc analysis indicated that gorillas and orangutan had the significant higher values than all other species, though they did not differ from each other. Furthermore, humans, chimpanzees and bonobos had significantly higher values than all Old World monkeys and lesser ape species but did not differ from each other. Finally, gibbons and baboons had significantly higher values than vervet, rhesus and bonnet monkeys.

We also analyzed species mean Percent_CS using phylogenetic ANOVA, comparing monkeys versus apes. When humans are included in the ape group, the difference is not significant ($F = 6.82$, $p = 0.30$); however, when humans are removed from the ape group, then the difference approaches significance ($F = 16.46$, $p < 0.02$). These results indicate that apes, which have a larger brain size, also tend to have a larger proportion of CS surface area relative to the rest of the folded cerebral cortex, although humans depart from this trend in having a relatively smaller CS surface area as compared to great apes.

We examined the scaling of CS surface area against the rest of the folded cortical surface area using species mean data. When humans are not included, both ordinary least squares and PGLS regressions demonstrate a positive allometric relationship (OLS: slope = 1.29, 95% CI = 1.12 – 1.46, $r^2 = 0.98$, $p < 0.001$; PGLS: slope = 1.20, 95% CI = 1.00 – 1.39, $r^2 = 0.96$, $p < 0.001$). Human values for CS surface area fall below the predictions based on the nonhuman primate scaling relationship (Figure 6). Consequently, when humans are included in the analysis the scaling exponent is reduced and includes isometry within the 95% confidence intervals (OLS: slope = 1.12, 95% CI = 0.93 – 1.31, $r^2 = 0.95$, $p < 0.001$; PGLS: slope = 0.95, 95% CI = 0.73 – 1.17, $r^2 = 0.92$, $p < 0.001$).

Overall Cortical Folding of the Central Sulcus

In the next analysis, we examined species differences in folding of the CS along the dorsal-ventral axis using the parameterization methods of BrainVISA described above. As can be seen in Figure 7, in humans and great apes, the depth of the middle portion of the CS is small relative to the adjacent dorsal and ventral regions. This pattern of distinct dorsal-ventral variation in CS depth, however, is absent in gibbons and the Old World monkey species and is likely attributable to the increased size of the PPFM in great apes and humans compared to other primates.

Variability in the PPFM Between Great Apes and Humans

For the PPFM_max measure, significant species differences were found between apes and humans ($F_{(4, 69)} = 4.87$, $p < 0.008$). The mean PPFM_max values for each species are shown in Figure 8 and these findings reflect the dorsal-ventral CS patterns illustrated in Figure 7. The mean PPFM_max was significantly smaller in humans and orangutans compared to bonobos but not chimpanzees and gorillas. Thus, despite having a brain that is three times larger than the great apes in absolute size, the PPFM_max depth is small in humans compared to most other great apes, with the exception of orangutans.

Discussion

Three main findings emerged from this study. First, after the split between Old Worlds monkeys and with lesser apes, CS surface area increased in size relative to cortical surface area up to the point of the split between the genus *Pan* and *Homo*. At that point in primate evolution, the total CS surface area and corresponding motor-hand region, like primary sensory cortices [de Sousa et al. 2010] did not keep pace with the expansion of other cortical association regions [Sherwood et al. 2012], resulting in humans having a relatively small CS surface area after adjusting for total folded cortical surface area.

Second, great apes and humans show a distinct dorsal-ventral pattern in CS folding compared to lesser apes and Old World monkeys. Specifically, in great apes and humans, the central portion of the CS is marked by a shallow folding while being preceded and followed by deep folding (see Figure 7). This pattern of distinct dorsal-ventral variation in CS depth is likely attributable to the increased size of the PPFM in great apes and humans compared to other primates. Because the CS has to fold over the PPFM, it might further explain the anatomical presence of the KNOB or motor-hand area in great apes and humans as has been previously described in these species [Hopkins and Pilcher 2001; Yousry et al. 1997].

Third, the mean PPFM_max depth was significantly smaller in humans and orangutans compared to gorillas, chimpanzees, and bonobos. Paradoxically, the lower PPFM_max values may reflect increased size of the PPFM in humans and orangutans compared to the other African great apes. Assuming that the CS has to fold over the PPFM, the shallower central depths may reflect that presence of a larger buried PPFM gyrus, which subsequently inhibits the CS from folding inward in that portion of the precentral gyrus. In short, because the PPFM is larger and projects closer to the cortical surface, the sulcus is inhibited from forming a deeper fold.

With respect to the overall CS surface area, there do not appear to be any distinct changes in the size and folding as a consequence of the evolution of increased specializations in the functional use of the hands for tool manufacture in hominins [Tocheri et al. 2008]. Thus, it does not appear that humans have a relatively large or more gyrified CS compared to other primates. We suggest that, instead of increased expansion of the CS, what likely happened after the split between the common ancestor of humans, chimpanzees, and bonobos was increasing expansion in other cortical regions, particularly within association regions, including the premotor and prefrontal cortex. This expansion would result in the increased connectivity and gyrification found in the frontal lobe regions in humans compared to nonhuman primates. Several bodies of research support this interpretation: First, Rilling and Insel (1999) and others [Armstrong et al. 1993] have reported that humans are significantly more gyrified in the prefrontal cortex, after adjusting for overall brain size, than other primates. Second, a number of authors have reported that humans have a disproportionally higher amount of white compared to grey matter in the premotor and prefrontal cortex when compared to other primate species [Rilling and Insel 1999b; Rilling and Insel 1999a; Schoenemann et al. 2005; Smaers et al. 2011]. Presumably the increasing white matter reflects increased connectivity between prefrontal and premotor cortex with other cortical regions in the brain. Third, cytoarchitectonic analyses of several cortical regions in humans and great apes have revealed significant changes in important premotor and prefrontal cortical regions. For example, Schenker et al. [2010] found that Brodmann's area 44 and 45, constituent parts of Broca's area, was nearly 7 times larger in humans compared to chimpanzees. Similarly, Semendeferi and colleagues (2001) found that area 10, a portion of prefrontal cortex thought to be involved in long-term motor planning, was 6.6 times larger in humans compared to other apes [Semendeferi et al. 2001]. In contrast, area 13 within the prefrontal cortex which is part of the limbic system, was only 1.5 time larger in humans compared to great apes [Semendeferi et al. 1998].

The relatively small CS surface area in humans as compared to great apes is consistent with some reports that humans have a relatively small precentral gyrus as well as Brodmann's area 4. For example, based on previously published data, Schoenemann [2006] reported that human primary motor cortex was only 33% as large as would be predicted for primate of our brain size, indicating that it is relatively small as compared to other neocortical regions. Similarly, Semendeferi et al. (2002) reported that the human precentral gyrus volume, as a percentage of total brain, was within the same range as those reported in great apes but that the orangutans looked more similar to humans than chimpanzees, bonobos and gorillas.

As noted above, within the CS, there are species differences in the dorsal-ventral folding patterns with the human and ape clade showing the presence of a shallow central region, presumably due to the fact that the CS must fold over the buried PPFM gyrus that connects the pre- and post-central gyri. When considering the magnitude of folding of the central CS region, as reflected by the PPFM_max value, we also found that humans and orangutans had significantly smaller PPFM_max values than gorillas, chimpanzees and bonobos. Assuming that the variation in central CS depths (i.e., the SP, PPFM and IP measures) reflects the need for CS to fold over the buried PPFM gyrus, one interpretation of these results is that the smaller PPFM_max values reflect a larger PPFM buried gyrus. In other words, smaller PPFM_max values reflect a larger PPFM gyrus. If this is the case, humans and orangutans have large (in absolute terms) PPFM gyri, which would suggest that they have greater connectivity and presumably sensory-motor integration between the pre- and post-central gyri. In the case of humans, this might reflect an adaptation for bipedalism and increased use of the hands for tool-use and other manual functions, which would be consistent with our hypothesis. Of course, the remaining challenge is the interpretation of the orangutan results in the context of the findings in humans, gorillas, chimpanzees and bonobos since they are the least terrestrial living species of the great apes. We would suggest that one possible explanation for the more human-like PPFM in orangutans is their arboreal habitat and the need for power grasping with both the hands and feet for locomotion. In this scenario, the central CS region between the SP and IP of the orangutan brain may control not just motor functions of the hands but also the feet and this requires greater integration of the sensory and motor regions leading to increased size of the PPFM gyrus. In the case of humans, they may also have a similarly large PPFM gyrus but it may solely reflect sensory-motor integration of the motor functions of the hands and individual digits. This hypothesis is speculative but, in principle, could be tested using modern functional imaging technologies that focus on identifying the cortical representation of hand and feet movements in different primate species [Ehrsson et al. 2000; Hopkins et al. 2010b].

There are at least two limitations to this study. First, we used both post-mortem and *in vivo* imaged brains in this study and this variable was not balanced within or between species. However, we do not believe this influenced the results in any substantive way. Indeed, because we used adjusted CS measures based on individual data obtained from the same brains, this presumably did not unfairly bias the data in any significant way. However, we also performed a follow up analysis comparing the raw and adjusted CS measures from the chimpanzee sample, which was comprised of 10 post-mortem and 9 *in vivo* scans. The descriptive data are shown in Table 1. For the raw CS surface area, CS mean depth and total

fold area, the values were significantly larger in the cadaver compared to *in vivo* scans; however, for the adjusted scores, no significant differences were found between the post-mortem and *in vivo* specimens. Because the adjusted scores were the primary dependent measures of interest, we do not believe that the variation in scanning protocols and magnets had any significant impact on our findings.

Second, we did not examine asymmetries in the CS surface area and depth but rather used averages between the two hemispheres. Although asymmetries could have been assessed, comparing the findings among species would be difficult for a number of reasons. Among them, because of the rather small sample sizes within some species, we would be underpowered in detecting significant population-level asymmetries. This type of analysis is further complicated by the fact that we did not have phenotypic data on behavior, such as hand preferences, in many of the subjects. Studies in humans, chimpanzees and, to a lesser extent monkeys, have found the depth of the left and right CS differs between right- and left-handed subjects [Amunts et al. 1996; Hopkins and Cantalupo 2004; Phillips and Sherwood 2005]. A comparison of asymmetries in the CS would be of interest given the known phylogenetic differences in hand preferences that have been reported in nonhuman primates for certain tasks [Hopkins et al. 2011; Westergaard et al. 1998; Westergaard et al. 2001]; however, this question remains for future study if sufficient sample sizes within different species can be obtained.

In summary, the current study shows that the surface area, shape, and folding pattern of the CS changed during Old World anthropoid primate evolution, presumably to reflect the increasing importance of somatosensory and motor integration of hand functions. Notably, as brain size increased after the split between lesser and great apes, folding in the CS had to accommodate the increasing size of the PPFM which resulted in the anatomical formation of the motor-hand area or KNOB that can be visibly seen on the surface projection of the central sulcus. Among apes, humans and orangutan have a relatively small PPFM_max when considered within the context of the overall surface area of the CS and these may reflect specific adaptations to bipedalism as well as motor control of the hands and feet.

Acknowledgments

This research was supported by NIH grants NS42867, NS73134**,** HD56232 and HD60563 and Cooperative Agreement RR15090. Additional support was provided by Fondation Fyssen and by French National Research Agency (ANR) grant (LangPrimate ANR-12-PDOC-0014_01) to Dr. Adrien Meguerditchian**,** ANR grant (BrainMorph, ANR-09-BLAN-0038-01) to Dr. Olivier Coulon**,** NIH grants MH084980 (AJB, PJP), AA013973 (MLL), Translational Center for Neurobehavioral Alcohol Research AA017056 (AJB, PJP), NIH Roadmap for Biomedical Research grant U54 RR021813 to Scott Fears and Roger Woods, and the James S. McDonnell Foundation (Grant numbers 22002078 and 220020293). We would like to thank Yerkes National Primate Research Center and the Wake Forest Primate Center and their respective veterinary staff for assistance in MR imaging. Further assistance was appreciated from Jamie Russell, Jennifer Schaeffer, Jared Taglialatela, Joseph McIntyre, Christopher Corcoran, Jeremy Bailoo, and Cynthia Lees. American Psychological Association guidelines for the treatment of animals were followed during all aspects of this study. Assistance in graphic editing by K. McKee is appreciated.

References

Alkadhi H, Kollias SS. Pli de passage fronto-parietal moyen of broca separates the motor homoculus. American Journal of Neuroradiology. 2004; 25

Amunts K, Schlaug G, Schleicher A, Steinmutz H, Drabinghaus A, Roland P, Zilles K. Asymmetry in the human motor cortex and handedness. Neuroimage. 1996; 4:216–222. [PubMed: 9345512]

Armstrong E, Zilles K, Schleicher A. Cortical folding and the evolution of the human brain. J Hum Evol. 1993; 20:341–348.

Bailey, P.; von Bonin, G.; McCulloch, WS. The isocortex of the chimpanzee. Urbana-Champaign: University of Illinois Press; 1950.

Boling W, Olivier A, Bittar R, Reutens D. Localization of hand motor activation in broca's *pli de passage moyen*. J Neurosurg. 1999; 91:903–910. [PubMed: 10584833]

Boroojerdi B, Foltys H, Krings T, Spetzger U, Thron A, Topper R. Localization of the motor hand area using transcranial magnetic stimulation and functional magnetic resonance imaging. Clin Neurophysiol. 1999; 110:699–704. [PubMed: 10378741]

Bradshaw, JL. Human evolution: A neuropsychological perspective. Hove, U.K.: Psychology Press; 1997.

Castiello U. The neuroscience of grasping. Nature Reviews: Neuroscience. 2005; 6:726–736.

Caulo M, Briganti C, Mattei PA, Perfetti B, Ferretti A, Romani GL, Tartaro A, Colosimo C. New morphological variants of the hand motor cortex as seen with mr imaging in a large study population. American Journal of Neuroradiology. 2007; 28:1480–1485. [PubMed: 17846195]

Christel, MI. Catarrhine primates grasping small objects: Techniques and hand preferences. In: Anderson, JR.; Roeder, JJ.; Thierry, B.; Herrenschmidt, N., editors. Current primatology vol iii: Behavioral neuroscience, physiology and reproduction. Strasbourg: Universite Louis Pasteur; 1994. p. 37-49.

Connolly, KJ. The psychobiology of the hand. London: Lavenham Press; 1998.

Corballis, MC. From hand to mouth: The origins of language. Princeton, NJ: Princeton University Press; 2002.

Coulon O, Clouchoux C, Operato G, Dauchot K, Sirigu A, Anton JL. Cortical localization via surface parameterization: A sulcus-based approach. Neuroimage. 2006; 31:S46.

Cykowski MD, Coulon O, Kochunov PV, Amunts K, Lancaster JL, Laird AR, Glahn C, Fox PT. The central sulcus: An observer-independent characterization of sulcal landmarks and depth asymmetry. Cerebral Cortex. 2008; 18:1999–2009. [PubMed: 18071195]

Davatzikos C, Bryan RN. Morphometric analysis of cortical sulci using parametric ribbons: A study of the central sulcus. Journal of Computer Assisted Tomography. 2002; 26:298–307. [PubMed: 11884791]

de Sousa AA, Sherwood CC, Mohlberg A, Amunts K, Schleicher A, MacLeod CE, Hof PR, Frahm H, Zilles K. Hominoid visual brain structure volumes and the position of the lunate sulcus. J Hum Evol. 2010; 58:281–292. [PubMed: 20172590]

Ehrsson HH, Fagergren A, Jonsson T, Westling G, Johansson RS, Forssberg H. Cortical activity in precision- versus power-grip tasks: An fmri study. Journal of Neurophysiology. 2000; 83:528–536. [PubMed: 10634893]

Fears SC, Melega WP, Service SK, Lee C, Chen K, Tu ZW, Jorgensen MJ, Fairbanks LA, Cantor RM, Freimer NB, Woods RP. Identifying heritable brain phenotypes in an extended pedigree of vervet monkeys. J Neurosci. 2009; 29:2867–2875. [PubMed: 19261882]

Felsenstein J. Phylogenies and the comparative method. The American Naturalist. 1985; 125:1–15.

Foundas AL, Hong KW, Leonard CM, Heilman KM. Hand preference and magnetic resonance imaging asymmetries of the central sulcus. Neuropsychiatry, Neuropsychology and Behavioral Neuroscience. 1998; 11:65–71.

Garland T, Dickerman AW, Janis CM, JA J. Phylogenetic analysis of covariance by computer stimulation. Syst Biol. 1993; 42:265–292.

Grafen A. The phylogenetic regression. Philosophical Transactions of the Royal Society B: Biological Sciences. 1989; 326:119–157.

Hopkins WD, Pilcher DL. Neuroanatomical localization of the motor hand area with magnetic resonance imaging: The left hemisphere is larger in great apes. Behav Neurosci. 2001; 115:1159–1164. [PubMed: 11584929]

Hopkins WD, Cantalupo C. Handedness in chimpanzees is associated with asymmetries in the primary motor but not with homologous language areas. Behav Neurosci. 2004; 118:1176–1183. [PubMed: 15598127]

Hopkins WD, Coulon O, Mangin JF. Observer-independent characterization of sulcal landmarks and depth asymmetry in the central sulcus of the chimpanzee brain. Neuroscience. 2010a; 171:544–551. [PubMed: 20813164]

Hopkins WD, Taglialatela JP, Russell JL, Nir T, Schaeffer JA. Cortical representation of lateralized grasping in chimpanzees (pan troglodytes): A combined mri and pet study. PlosOne. 2010b; 5:1–10.

Hopkins WD, Phillips KA, Bania A, Calcutt SE, Gardner M, Russell JL, Schaeffer JA, Lonsdorf EV, Ross S, Schapiro SJ. Hand preferences for coordinated bimanual actions in 777 great apes: Implications for the evolution of handedness in hominins. J Hum Evol. 2011; 60

Kloppel S, Mangin JF, Vongerichten A, Frackowiak RSJ, Siebner HR. Nurture versus nature: Long-term inpact of forced right-handedness on structure of pericentral cortex and basal ganglia. The Journal of Neuroscience. 2010; 30:3271–3275. [PubMed: 20203186]

Li L, Preuss TM, Rilling JK, Hopkins WD, Glasser MF, Kumar B, Nana R, Zhang X, Hu X. Chimpanzee pre-central corticospinal system asymmetry and handedness: A diffusion magnetic reonance imaging study. PlosOne. 2009; 5:e12886.

Mangin JF, Frouin V, Bloch I, Regis J, Lopez-Krahe J. From 3d magnetic resonance imaging to structural representations of the cortex topography using topology preserving deformations. Journal of Mathematical Imaging and Vision. 1995; 5:297–318.

Mangin, JF.; Regis, J.; Frouin, V. Workshop on Mathematical Methods in Biomedical Image Analysis. San Francisco, CA: IEEE Press; 1996. Shape bottlenecks and conservative flow systems; p. 319-328.

Mangin, JF.; Coulon, O.; Frouin, V. Robust brain segmentation using histogram scale-space analysis and mathematical morphology. In: Colchester, A.; Delp, S., editors. Medical image computing and computer-assisted intervention-miccai'98. Vol. 1496. Boston, MA: Springer-Verlag; 1998. p. 1230-1241.

Mangin, JF. MMBIA. Hilton Head, South Carolina: IEEE Press; 2000. Entropy minimization for automatic correction of intensity nonuniformity; p. 162-169.

Mangin JF, Riviere D, Cachia A, Duchesnay E, Cointepas Y, Papadopoulos-Orfanos D, Collins DL, Evans AC, Regis J. Object-based morphometry of the cerebral cortex. Medical Imaging. 2004; 23:968–982. [PubMed: 15338731]

Martins EP, Hansen TF. Phylogenies and the comparative method: A general approach to incorporating phylogenetic information into the analysis of interspecific data. The American Naturalist. 1997; 149:646–667.

Marzke, MW. Evolution of the hand and bipedality. In: Peters ALC, R., editor. Handbook of human symbolic evolution. New York: Wiley-Blackwell; 1996. p. 126-154.

Marzke MW. Precision grips, hand morphology, and tools. Am J Phys Anthropol. 1997; 102:97–110.

Orme D. The caper package: Comparative analysis of phylogenetics and evolution in r. 2012 In.

Penfield W, Boldrey E. Somatic motor and sensory representation in the cerebral cortex of man as studied by electrical stimulation. Brain. 1936; 60:389–443.

Petrides M, Cadoret G, Mackey S. Orofacial somatomotor responses in the macaque monkey homologue of broca's area. Nature. 2005; 435:1235–1238. [PubMed: 15988526]

Phillips K, Sherwood CC. Primary motor cortex asymmetry correlates with handedness in capuchin monkeys (*cebus apella*). Behav Neurosci. 2005; 119:1701–1704. [PubMed: 16420175]

Pizzella V, Tecchio F, Romani GL, Rossini PM. Functional localization of the sensory hand area with respect to the motor central gyrus knob. Neuroreport. 1999; 10:3809–3814. [PubMed: 10716214]

Pouydebat W, Gorce P, Coppens Y, Bels V. Biomechanical study of grasping according to the volume of the object: Human versus non-human primates. J Biomech. 2009; 42:266–272. [PubMed: 19100551]

Revell LJ. Phytools: An r package for comparative biology (and other things). Methods in Ecology and Evolution. 2011; 3:217–223.

Rilling JK, Insel TR. Differential expansion of neural projection systems in primate brain evolution. Neuroreport. 1999a; 10:1453–1459. [PubMed: 10380962]

Rilling JK, Insel TR. The primate neocortex in comparative perspective using magnetic resonance imaging. J Hum Evol. 1999b; 37:191–223. [PubMed: 10444351]

Rogers J, Kochunov PV, Zilles K, Shelledy W, Lancaster JL, Thompson P, Duggirala R, Blangero J, Fox PT, Glahn DC. On the genetic architecture of cortical folding and brain volume in primates. Neuroimage. 2010; 53:1103–1108. [PubMed: 20176115]

Sastre-Janer FA, Regis J, Belin P, Mangin JF, Dormont D, Masure MC, Remy P, Frouin V, Samson Y. Three-dimensional reconstruction of the human central sulcus reveals a morphological correlate of the hand area. Cerebral Cortex. 1998; 8:641–647. [PubMed: 9823485]

Schenker NM, Hopkins WD, Spocter MA, Garrison A, Stimpson CD, Erwin JM, Hof PR, Sherwood CC. Broca's area homologue in chimpanzees (*pan troglodytes*): Probabilistic mapping, asymmetry and comparison to humans. Cerebral Cortex. 2010; 20:730–742. [PubMed: 19620620]

Schoenemann PT, Sheehan MJ, Glotzer LD. Prefrontal white matter volume is disproportionately larger in humans than in other primates. Nat Neurosci. 2005; 8:242–252. [PubMed: 15665874]

Schoenemann PT. Evolution of size and functional areas of the human brain. Annu Rev Anthropol. 2006; 35:379–406.

Semendeferi K, Armstrong E, Schleicher A, Zilles K, Van Hoesen GW. Limbic frontal cortex in hominoids: A comparative study of area 13. Am J Phys Anthropol. 1998; 106:129–155. [PubMed: 9637180]

Semendeferi K, Armstrong E, Schleicher A, Zilles K, Van Hoesen GW. Prefrontal cortex in humans and apes: A comparative study of area 10. Am J Phys Anthropol. 2001; 114:224–241. [PubMed: 11241188]

Sherwood CC, Holloway RL, Erwin JM, Hof PR. Cortical orofacial motor representation in old word monkeys, great apes and humans: Ii. Sterological analysis of chemoarchitecture. Brain, Behavior and Evolution. 2004; 63:82–106.

Sherwood CC, Wahl E, Erwin JM, Hof PR, Hopkins WD. Histological asymmetries of primary motor cortex predicts handedness in chimpanzees (*pan troglodytes*). J Comp Neurol. 2007; 503:525–537. [PubMed: 17534947]

Sherwood CC, Duka T, Stimpson CD, Schenker NM, Garrison A, Schapiro SJ, Baze WB, McArthur MJ, Erwin JM, Hof PR, Hopkins WD. Neocortical synaptophysin asymmetry and behavioral lateralziation in chimpanzees (*pan troglodytes*). Eur J Neurosci. 2010; 31:1456–1464. [PubMed: 20384782]

Sherwood, CC.; Baurernfeind, AL.; Bianchi, S.; Raghanti, MA.; Hof, PR. Human brain evolution writ large and small. In: Hofman, MA.; Falk, D., editors. Prog brain res. Elsevier; 2012.

Smaers JB, Steele J, Case CR, Cowper A, Amunts K, Zilles K. Primate prefrontal cortex evolution: Humans brains are the extreme of a lateralzied ape trend. Brain, Behavior and Evolution. 2011; 77:67–78.

Team RDC. R: A language and environment for statisticl computing. 2011

Tocheri M, Orr CM, Jacofsky C, Marzke Mw. The evolutionary history of the hominin hand since the last common ancestor of *pan* and *homo*. J Anat. 2008; 212:544–562. [PubMed: 18380869]

Westergaard GC, Kuhn HE, Suomi SJ. Bipedal posture and hand preference in humans and other primates. J Comp Psychol. 1998; 112:56–63.

Westergaard GC, Lussier ID, Higley JD. Between-species variation in the development of hand preference among macaques. Neuropsychologia. 2001; 39:1373–1378. [PubMed: 11585604]

Young RW. Evolution of the human hand: The role of throwing and clubbing. J Anat. 2003; 202:165–174. [PubMed: 12587931]

Yousry TA, Schmid UD, Alkadhi H, Schmidt D, Peraud A, Buettner A, Winkler P. Localization of the motor hand area to a knob on the precentral gyrus. A new landmark. Brain. 1997; 120:141–157. [PubMed: 9055804]

Zilles K, Armstrong E, Moser KH, Schleicher A, Stephan H. Gyrification in the cerebral cortex of primates. Brain, Behavior and Evolution. 1989; 34:143–150.

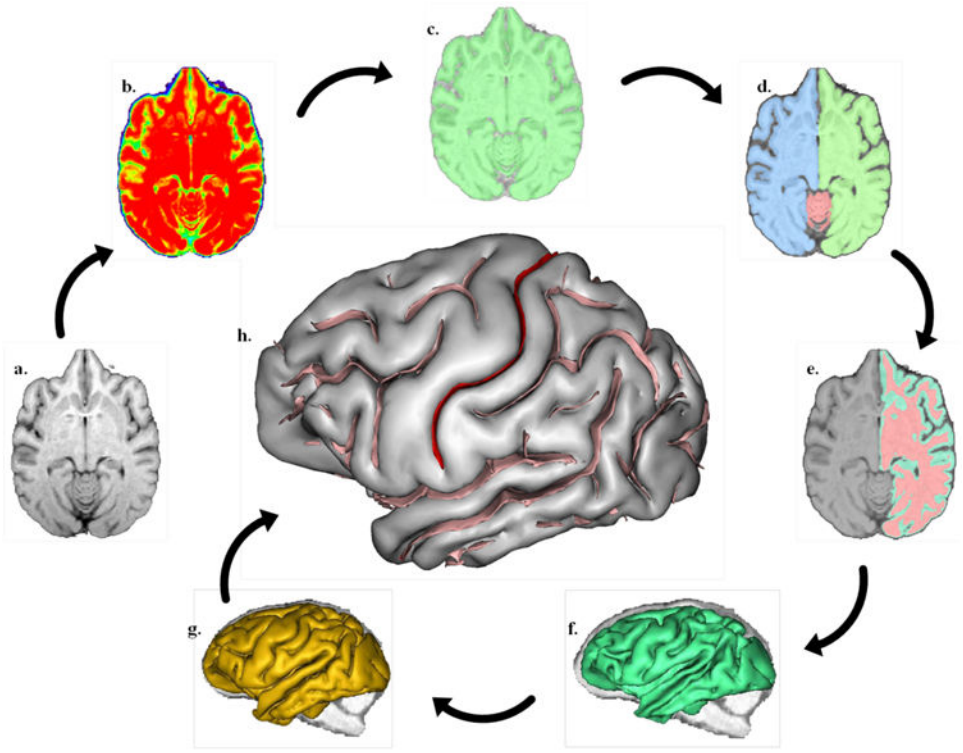

Figure 1.

BrainVISA's pipeline processing steps. a) MR image of a skull-stripped chimpanzee brain, b) stable tissue intensities after bias field correction, c) binary mask of the brain, d) split mask of left and right hemispheres and cerebellum, e) grey and white interface, f) A negative mould of the white matter, g) skeletonised mould of cortical folding, h) cortical fold graph of chimpanzee sulci with the central sulcus in red.

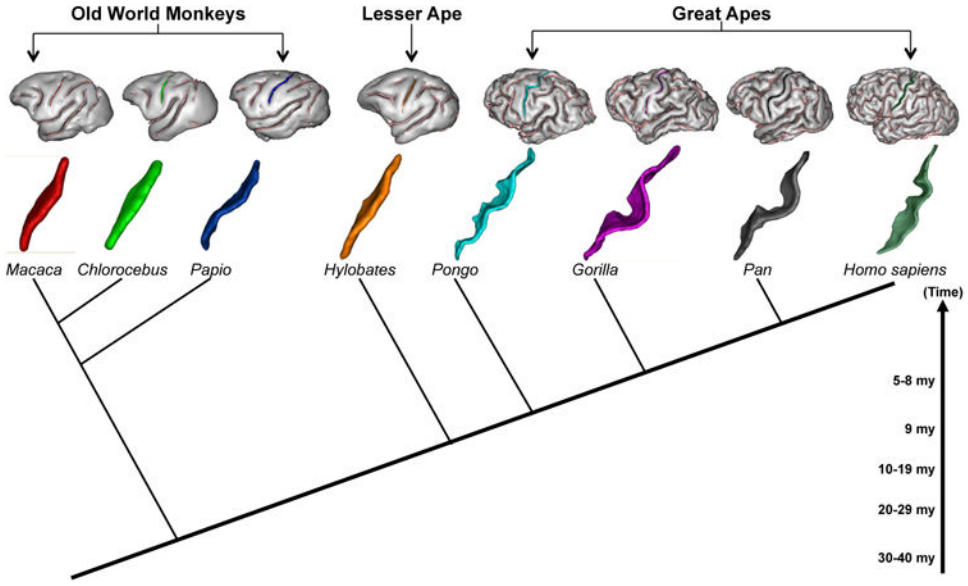

Figure 2.

Example 3D brain cortex reconstructions and extracted central sulci from representative primate species in the study along a phylogenetic timeline.

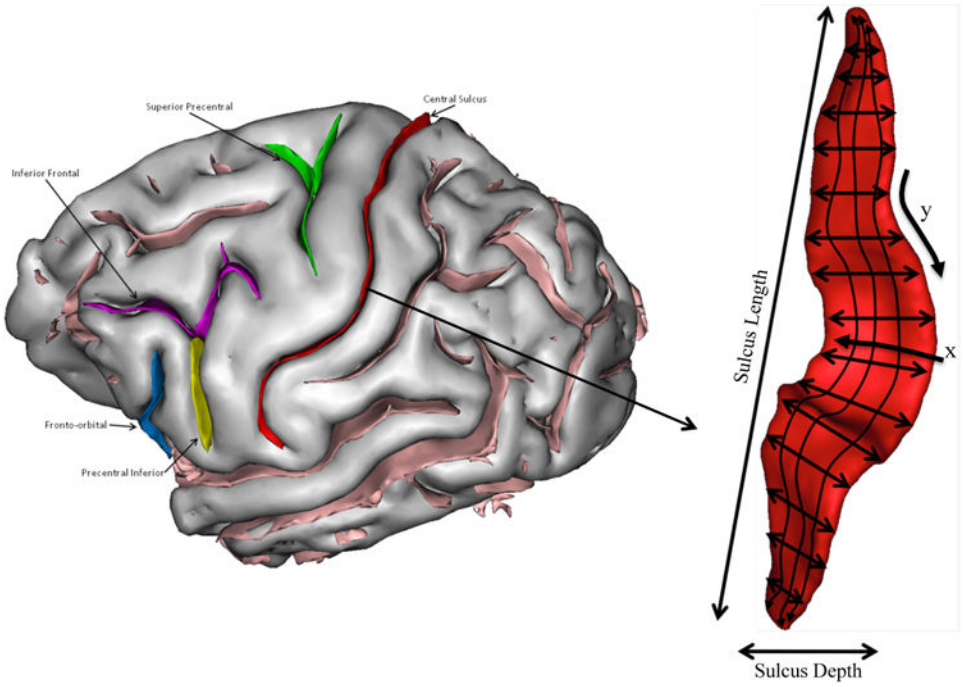

Figure 3.

Chimpanzee central sulcus labeled and extracted. The surface area and depth dimensions are shown in the extracted sulcus, as well as the x and y coordinates used for computing differences in cortical folding of the CS along the dorsal-ventral axis.

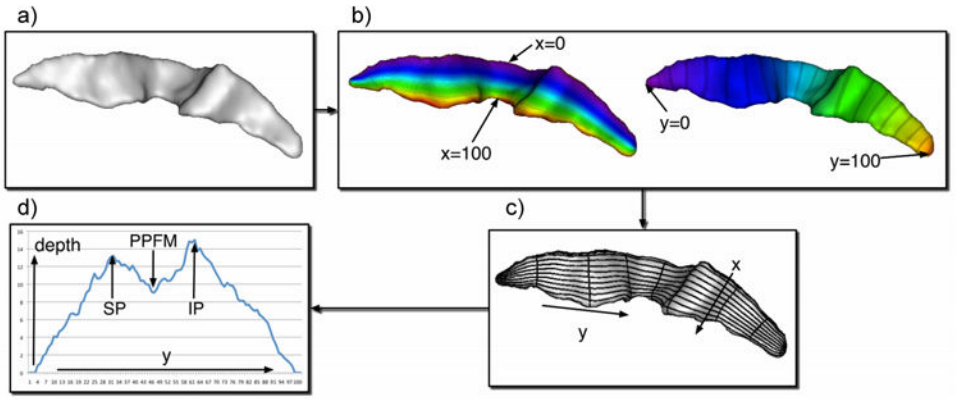

Figure 4.

a) Chimpanzee central sulcus b & c) the surface area and depth dimensions are shown in the extracted sulcus, as well as the x and y coordinates used for computing differences in cortical folding of the CS along the dorsal-ventral axis d) outputted data from CS parameterization. Depth of CS is plotted on ordinate and the y coordinate along the abscissa. SP = superior maximum CS depth before y coordinate 50, IP = maximum inferior depth after y coordinate 50, PPFM = pli-de-passage moyen parietale, which is the shallowest CS depth measure between the SP and IP y coordinates.

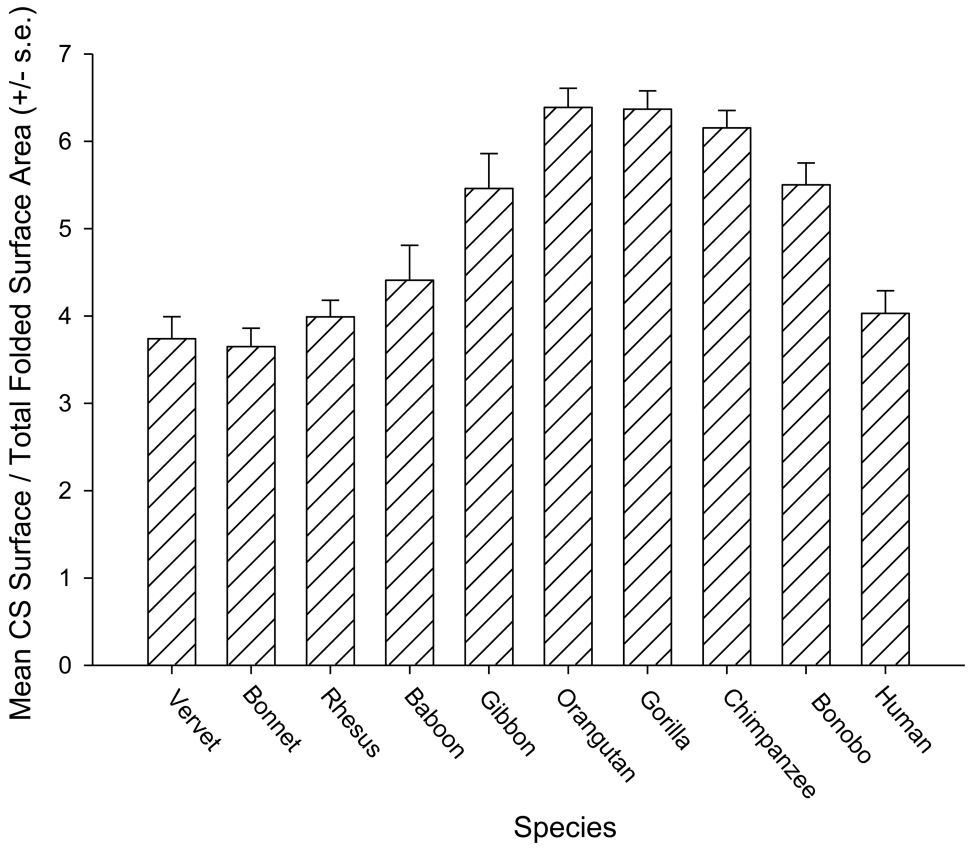

Figure 5.

Mean central sulcus (CS) surface area (± s.e.) as a percentage of total brain surface in 10 primate species.

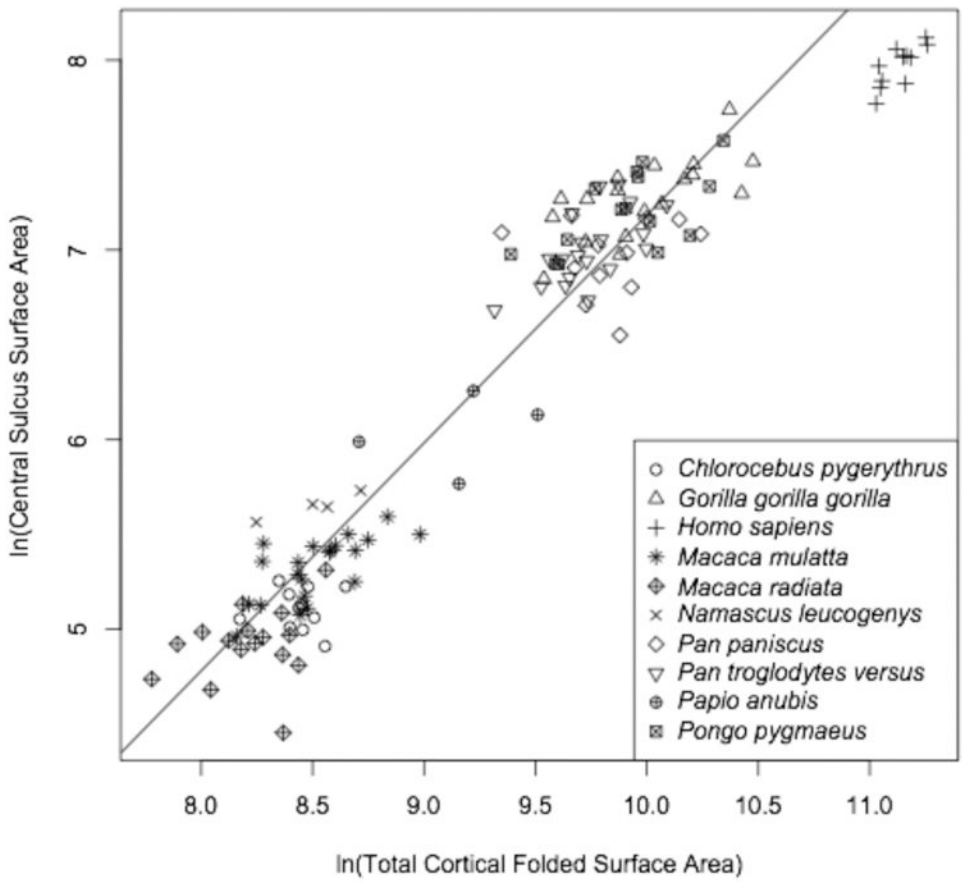

Figure 6.

Plot of CS surface area regressed against total cortical folded surface area in primates. All individual data from each species are plotted. The PGLS regression line shown was calculated based on species mean data from the total primate sample, excluding humans.

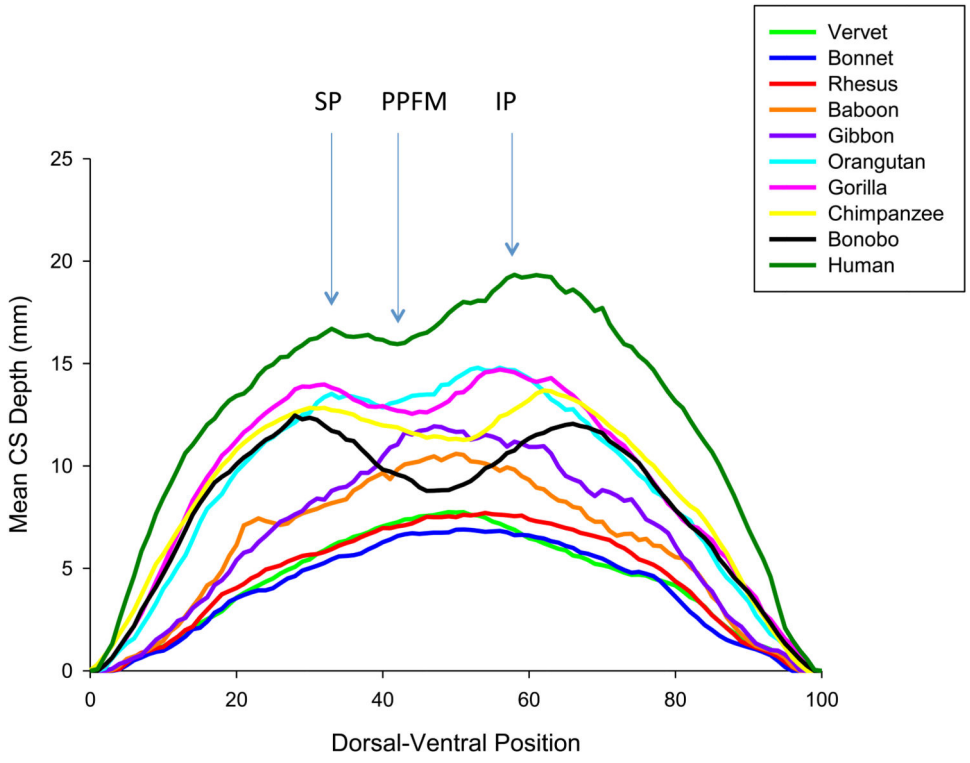

Figure 7.

Mean central sulcus (CS) depth along the dorsal to ventral plane in the 10 primate species. SP = deepest superior point, PPFM = shallowest point between SP and IP, IP = deepest inferior point.

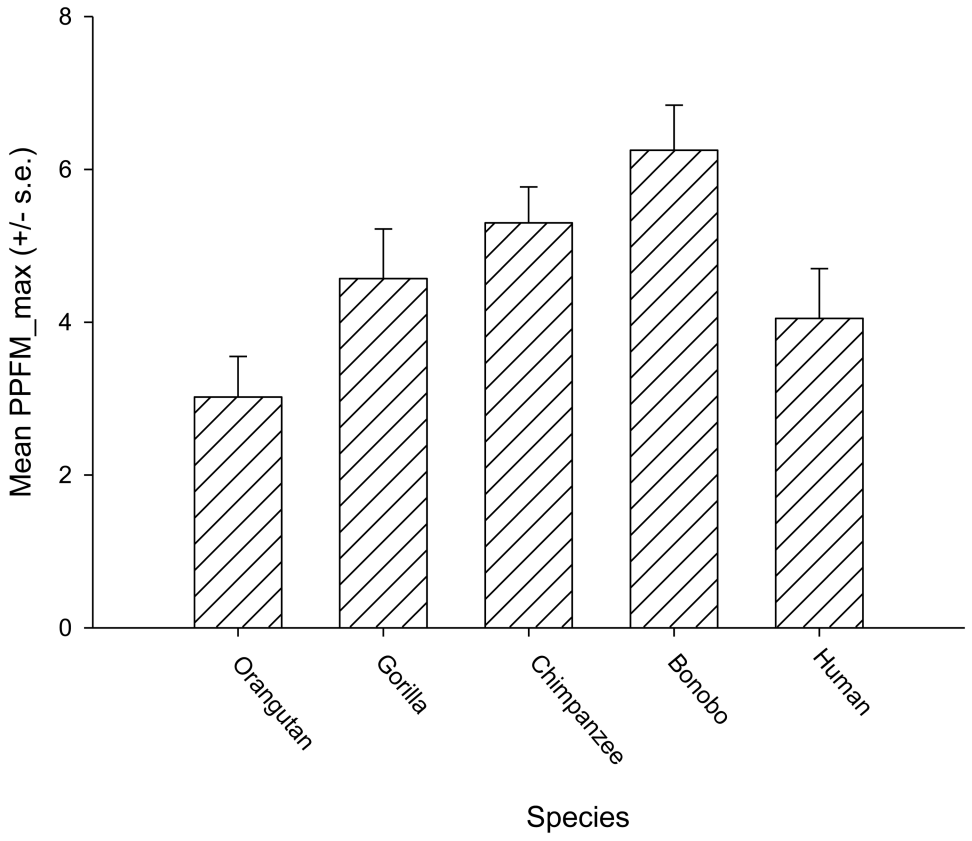

Figure 8.
Mean PPFM_max (± s.e.) in humans and great apes.

Table 1

	Post-Mortem	***In Vivo***	**F**
CS Surface Area	1248.78	989.14	9.26*
CS Depth	10.15	8.62	9.61*
Total Cortical Fold	20465.17	16193.43	13.26*
Percent CS/Total Fold	6.7%	6.0%	2.86
Percent PPFM/Total CS	28.9%	34.6%	2.12

Surface area measures are in mm^2 and depth measures in are mm.

* indicates $p < .05$.